

Experimental and Computational Study of the Bonding Properties of Mixed Bis–Ylides of Phosphorus and Sulfur

Elena Serrano,[†] Rafael Navarro,[†] Tatiana Soler,[‡] Jorge J. Carbó,^{*,§} Agustí Lledós,^{||} and Esteban P. Urriolabeitia^{*,†}

[†]Departamento de Compuestos Organometálicos, Instituto de Ciencia de Materiales de Aragón, CSIC-Universidad de Zaragoza, E-50009 Zaragoza, Spain, [‡]Servicios Técnicos de Investigación, Facultad de Ciencias Fase II, 03690 San Vicente de Raspeig, Alicante, Spain, [§]Departament de Química Física i Inorgànica, Universitat Rovira i Virgili, 43007 Tarragona, Spain, and ^{||}Departament de Química, Edifici C.n., Universitat Autònoma de Barcelona, 08193 Bellaterra, Barcelona, Spain

Received April 21, 2009

The reactivity of the known ylide-sulfonium salt $[\text{Ph}_3\text{P}=\text{CHC}(\text{O})\text{CH}_2\text{SMe}_2]\text{Br}$ **1** and the new ylide-sulfide $[\text{Ph}_3\text{P}=\text{CHC}(\text{O})\text{CH}_2\text{SMe}]$ **2** toward Pd^{II} complexes has been studied. Compound **1** reacts with $\text{PdCl}_2(\text{NCMe})_2$ and NEt_3 to give *cis*- $[\text{PdCl}_2[\text{Ph}_3\text{PCHC}(\text{O})\text{CHSMe}_2-\kappa\text{-C,C}]]$ **3**, which is obtained selectively as the meso diastereoisomer (*RS/SR*). The reactivity of **3** has been studied, and shows the stability of the bis-ylide unit. However, reflux in NCMe of $[\text{PdCl}(\text{PPh}_3)-[\text{Ph}_3\text{PCHC}(\text{O})\text{CHSMe}_2-\kappa\text{-C,C}]]\text{ClO}_4$ **6** promotes orthopalladation and affords $[\text{PdCl}(\text{PPh}_3)(\text{C}_6\text{H}_4\text{-2-PPH}_2\text{CHC}(\text{O})\text{CH}_2\text{SMe}_2-\kappa\text{-C,C})]\text{ClO}_4$ **12**, which is characterized by X-ray methods. Density functional theory (DFT) and Bader's Atoms in Molecules (AIM) studies on S-ylides, mixed P–S bis–ylides, and the corresponding Pd complexes have been performed. Free S-ylides show strong conformational preferences, which lies with the establishment of a set of cooperative intramolecular interactions of weak strength: the 1,4-S···O interactions and the 1,6-C–H···O H-bonds between the protons of the methyl substituents and the carbonyl oxygen was fully characterized for the first time. For free mixed P–S bis-ylides, an additional 1,4-P···O intramolecular interaction of moderate strength was characterized. These interactions play a key role in determining the preferred conformations, which then are transferred to the complexes, explaining the observed diastereoselectivity in complex **3**. The ylide–sulfide **2** reacts with $\text{PdCl}_2(\text{NCMe})_2$ and NEt_3 affording $[\text{Pd}(\text{Cl})[\text{Ph}_3\text{PCHC}(\text{O})\text{CHSMe}]]_2$ **9**, which in turn reacts with PPh_3 giving $[\text{Pd}(\text{Cl})(\text{PPh}_3)[\text{Ph}_3\text{PCHC}(\text{O})\text{CHSMe}-\kappa\text{-C,C}]]$ **10**. The X-ray structure of **10** shows the anion $[\text{Ph}_3\text{PCHC}(\text{O})\text{CHSMe}]^-$ acting as a C,C–chelate. The bonding in **10** is produced with complete diastereoselectivity but, instead of the expected meso form, the d,l pair (*RR/SS*) is formed. This inversion is observed for the first time.

Introduction

The behavior of the ylides as ligands toward transition metals is a well established research area.^{1–14} During the last 40 years many different subjects have been developed, most

of them being comprehensively reviewed.¹ The variety of research lines covers from structural studies, such as the different bonding modes of the ylides as ligands,^{2,3} or particular reactivities such as their addition to multiple bonds,^{4,5} to practical processes^{6–9} some of them of industrial interest.⁷ Multidentate ylides are specially attractive because of the additional stabilization provided by the chelating effect, and different strategies have been developed: classical C,X (X = heteroatom) chelates^{9,10} orthometalated species¹¹ or multiylides^{12–14} are some approximations developed in this area. Among these interesting species, the synthesis and bonding properties of bis-ylides has been one of the most studied topics in our group,^{11f–11h,12h,13b–13f} because of two noteworthy reactions shown in Figure 1. The first one is that, in spite of the presence of two chiral centers in the free bis–ylide, only one diastereoisomer (the meso form) is obtained.^{11f–11h,12h,13b–13f} The second one is the isomerization of the chelating bis–ylides in the $[\text{Pd}(\text{Ph}_3\text{PCHC}(\text{O})\text{CHEZ}_n)]$ units ($\text{EZ}_n = \text{PR}_3, \text{NC}_5\text{H}_5$) into the orthometalated ligands $[\text{Pd}(\text{C}_6\text{H}_4\text{-2-PPH}_2\text{CHC}(\text{O})\text{CH}_2\text{EZ}_n)]$ through arylic

*To whom correspondence should be addressed. E-mail: j.carbo@urv.cat (J.J.C.), esteban@unizar.es (E.P.U.). Fax: +34976761187 (E.P.U.).

(1) For general reviews: (a) Johnson, A. W. In *Ylides and Imines of Phosphorus*; John Wiley&Sons: New York, 1993; Chapter 14. (b) Kolodiazny, O. I. In *Phosphorus Ylides*; Wiley-VCH: Weinheim, Germany, 1999. (c) Schmidbaur, H. *Acc. Chem. Res.* **1975**, *8*, 62. (d) Schmidbaur, H. *Angew. Chem., Int. Ed. Engl.* **1983**, *22*, 907. (e) Weber, L. *Angew. Chem., Int. Ed. Engl.* **1983**, *22*, 516. (f) Laguna, A.; Laguna, M. *J. Organomet. Chem.* **1990**, *394*, 743. (g) Vicente, J.; Chicote, M. T. *Coord. Chem. Rev.* **1999**, *193–195*, 1143. (h) Cristau, H. J. *Chem. Rev.* **1994**, *94*, 1299. (i) Belluco, U.; Michelin, R. A.; Mozzon, M.; Bertani, R.; Facchin, G.; Zanutto, L.; Pandolfo, L. *J. Organomet. Chem.* **1998**, *557*, 37. (j) Navarro, R.; Urriolabeitia, E. P. *J. Chem. Soc., Dalton Trans.* **1999**, 4111. (k) Urriolabeitia, E. P. *Dalton Trans.* **2008**, 5673. (l) Bertani, R.; Casarin, M.; Pandolfo, L. *Coord. Chem. Rev.* **2003**, *236*, 15. (m) Chauvin, R. *Eur. J. Inorg. Chem.* **2000**, 577. (n) Taillefer, M.; Cristau, H. *J. Top. Curr. Chem.* **2003**, *229*, 41. (o) Kuhn, P.; Sémeril, D.; Matt, D.; Chetcuti, M. J.; Lutz, P. *Dalton Trans.* **2007**, 515. (p) Cantat, T.; Mézailles, N.; Auffrant, A.; Le Floch, P. *Dalton Trans.* **2008**, 1957.

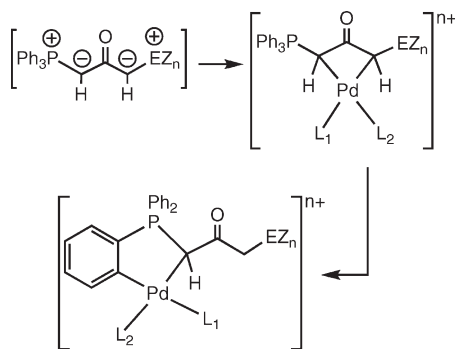


Figure 1. Remarkable reactivity of bis-ylides.

CH bond activation followed by an intramolecular acid–base reaction.^{11g,11h,13c}

With respect to the diastereoselective bonding of the ylides, we have shown that bis-ylides of phosphorus,^{13b,13c} arsenic, and nitrogen^{13d,13e} show the same selectivity, since in all cases the meso form is obtained (Figure 2). This is due to the presence of strong conformational preferences in free ligands favoring the cisoid form. However, although the experimental fact is the same (obtention of the meso form), the detailed analysis of the two systems reveals subtle differences. The study of these systems using density functional theory (DFT) methods and Bader's analysis of the charge density shows that in the case of P- or As-ylides a 1,4-P(As)···O

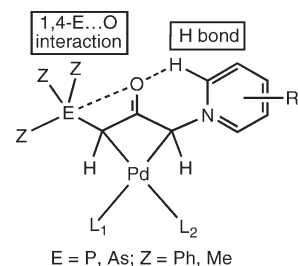


Figure 2. Conformational preferences on P, As and N bis-ylides.

intramolecular interaction is the one mainly responsible for the conformational preferences,^{13b–13c} while in the case of N-ylides a hydrogen bond of moderate strength plays the same role.^{13d,13e} We have reported very recently some examples of sulfur bis-ylides. Once again, we have observed the meso form of the bonded bis-ylide, both in the chelating and in the bridging modes.^{13f}

This paper describes the coordinating properties of mixed bis-ylides of phosphorus and sulfur of the type $[\text{Ph}_3\text{PCHC}(\text{O})\text{CHSM}_2]$ and those of the ylide–sulfide $[\text{Ph}_3\text{P}=\text{CHC}(\text{O})\text{CH}_2\text{SM}_2]$ which, in spite of their similarity, show a quite different behavior. Moreover, the study of the ligands

(2) For selected examples of complexes with C-bonded ylides, see: (a) Koezuka, H.; Matsubayashi, G.-E.; Tanaka, T. *Inorg. Chem.* **1974**, *13*, 443. (b) Koezuka, H.; Matsubayashi, G.-E.; Tanaka, T. *Inorg. Chem.* **1976**, *15*, 417. (c) Booth, B. L.; Smith, K. G. *J. Organomet. Chem.* **1981**, *220*, 219. (d) Saito, T.; Urabe, H.; Sasaki, Y. *Trans. Met. Chem.* **1980**, *5*, 35. (e) Usón, R.; Laguna, A.; Laguna, M.; Usón, A.; Jones, P. G.; Erdbrügger, C. F. *Organometallics* **1987**, *6*, 1778. (f) Facchin, G.; Bertani, R.; Calligaris, M.; Nardin, G.; Mari, M. *J. Chem. Soc., Dalton Trans.* **1987**, 1381. (g) Barco, I. C.; Falvello, L. R.; Fernández, S.; Navarro, R.; Urriolabeitia, E. P. *J. Chem. Soc., Dalton Trans.* **1998**, 1699. (h) Fernández, S.; García, M. M.; Navarro, R.; Urriolabeitia, E. P. *J. Organomet. Chem.* **1998**, *561*, 67. (i) Carbó, M.; Falvello, L. R.; Navarro, R.; Soler, T.; Urriolabeitia, E. P. *Eur. J. Inorg. Chem.* **2004**, 2338. (j) Pandolfo, L.; Paiaro, G.; Dragani, L. K.; Maccato, C.; Bertani, R.; Facchin, G.; Zanotto, L.; Ganis, P.; Valle, G. *Organometallics* **1996**, *15*, 3250. (k) Hirai, M.-F.; Miyasaka, M.; Itoh, K.; Ishii, Y. *J. Chem. Soc., Dalton Trans.* **1979**, 1200. (l) Bertani, R.; Casarin, M.; Ganis, P.; Maccato, C.; Pandolfo, L.; Venzo, A.; Vittadini, A.; Zanotto, L. *Organometallics* **2000**, *19*, 1373. (m) Spannenberg, A.; Baumann, W.; Rosenthal, U. *Organometallics* **2000**, *19*, 3991. (n) Vicente, J.; Chicote, M. T.; Guerrero, R.; Jones, P. G. *J. Am. Chem. Soc.* **1996**, *118*, 699. (o) Vicente, J.; Chicote, M. T.; Abrisqueta, M. D.; González-Herrero, P.; Guerrero, R. *Gold Bull.* **1998**, *31*, 126. (p) Hoover, J. F.; Stryker, J. M. *Organometallics* **1988**, *7*, 2082. (q) Ferguson, G.; Li, Y.; McAlees, A. J.; McCrindle, R.; Xiang, K. *Organometallics* **1999**, *18*, 2428. (r) Falvello, L. R.; Llusar, R.; Margalejo, M. E.; Navarro, R.; Urriolabeitia, E. P. *Organometallics* **2003**, *22*, 1132.

(3) For selected examples of complexes with O- or N-bonded ylides, see: (a) Albanese, J. A.; Staley, D. L.; Rheingold, A.; Burmeister, J. L. *Inorg. Chem.* **1990**, *29*, 2209. (b) Usón, R.; Forniés, J.; Navarro, R.; Espinet, P.; Mendivil, C. *J. Organomet. Chem.* **1985**, *290*, 125. (c) Falvello, L. R.; Fernández, S.; Navarro, R.; Urriolabeitia, E. P. *Inorg. Chem.* **1997**, *36*, 1136. (d) Falvello, L. R.; Fernández, S.; Navarro, R.; Pascual, I.; Urriolabeitia, E. P. *J. Chem. Soc., Dalton Trans.* **1997**, 763. (e) Facchin, G.; Zanotto, L.; Bertani, R.; Canoves, L.; Uguagliati, P. *J. Chem. Soc., Dalton Trans.* **1993**, 2871. (f) Belluco, U.; Michelin, R. A.; Bertani, R.; Facchin, G.; Pace, G.; Zanotto, L.; Mozzon, M.; Furlan, M.; Zangrando, E. *Inorg. Chim. Acta* **1996**, *252*, 355. (g) Falvello, L. R.; Fernández, S.; Navarro, R.; Urriolabeitia, E. P. *Inorg. Chem.* **1996**, *35*, 3064. (h) Soulvong, D.; Wieser, C.; Marcellin, M.; Matt, D.; Harriman, A.; Toupet, L. *J. Chem. Soc., Dalton Trans.* **1997**, 2257. (i) Falvello, L. R.; Ginés, J. C.; Carbó, J. J.; Lledós, A.; Navarro, R.; Soler, T.; Urriolabeitia, E. P. *Inorg. Chem.* **2006**, *45*, 6803. (j) Carbó, M.; Marín, N.; Navarro, R.; Soler, T.; Urriolabeitia, E. P. *Eur. J. Inorg. Chem.* **2006**, 4629.

(4) For selected examples of addition of ylides to olefins, see: (a) Vicente, J.; Chicote, M. T.; MacBeath, C.; Fernández-Baeza, J.; Bautista, D. *Organometallics* **1999**, *18*, 2677. (b) Vicente, J.; Chicote, M. T.; MacBeath, C.; Jones, P. G. *Organometallics* **2003**, *22*, 1843.

(5) For selected examples of addition of ylides to nitriles and isocyanides, see: (a) Vicente, J.; Chicote, M. T.; Fernández-Baeza, J.; Lahoz, F. J.; López, J. A. *Inorg. Chem.* **1991**, *30*, 3617. (b) Vicente, J.; Chicote, M. T.; Lagunas, M. C.; Jones, P. G. *Inorg. Chem.* **1995**, *34*, 5441. (c) Vicente, J.; Chicote, M. T.; Beswick, M. A.; Ramírez, M. C. *Inorg. Chem.* **1996**, *35*, 6592. (d) Michelin, R. A.; Facchin, G.; Braga, D.; Sabatino, P. *Organometallics* **1986**, *5*, 2265.

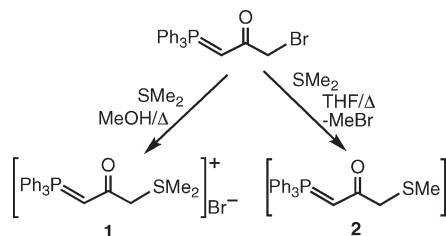
(6) For selected examples of addition of ylides as reducing agents, see: (a) Wagner, G.; Pakhomova, T. B.; Bokach, N. A.; Fraústo, J. J. R.; Vicente, J.; Pombeiro, A. J. L.; Kukushkin, V. Y. *Inorg. Chem.* **2001**, *40*, 1683. (b) Bokach, N. A.; Selivanov, S. I.; Kukushkin, V. Y.; Vicente, J.; Haukka, M.; Pombeiro, A. J. L. *Organometallics* **2002**, *21*, 3744. (c) Bokach, N. A.; Kukushkin, V. Y.; Haukka, M.; Fraústo, J. J. R.; Pombeiro, A. J. L. *Inorg. Chem.* **2003**, *42*, 3602.

(7) For selected examples of oxidative addition of ylides: Keim, W.; Kowaldt, F. H.; Goddard, R.; Krügger, C. *Angew. Chem., Int. Ed. Engl.* **1978**, *17*, 466.

(8) For selected examples of carbodiphosphoranes and related species, see: (a) Schmidbaur, H.; Zybill, C. E.; Müller, G.; Krüger, C. *Angew. Chem., Int. Ed. Engl.* **1983**, *22*, 729. (b) Petz, W.; Weller, F.; Uddin, J.; Frenking, G. *Organometallics* **1999**, *18*, 619. (c) Vicente, J.; Singhal, A. R.; Jones, P. G. *Organometallics* **2002**, *21*, 5887. (d) Petz, W.; Kutschera, C.; Neumüller, B. *Organometallics* **2005**, *24*, 5038. (e) Baldwin, J. C.; Kaska, W. C. *Inorg. Chem.* **1979**, *18*, 686. (f) Brownie, J. H.; Baird, M. C.; Schmid, H. *Organometallics* **2007**, *26*, 1433.

(9) For selected examples of chiral C,X-chelating ylides, see: (a) Viau, L.; Lepetit, C.; Commenges, G.; Chauvin, R. *Organometallics* **2001**, *20*, 808. (b) Zurawinski, R.; Donnadiu, B.; Mikolajczyk, M.; Chauvin, R. *Organometallics* **2003**, *22*, 4810.

(10) For selected examples of nonchiral C,X-chelating ylides, see: (a) Canac, Y.; Lepetit, C.; Abdalilah, M.; Duhayon, C.; Chauvin, R. *J. Am. Chem. Soc.* **2008**, *130*, 8406. (b) Vignolle, J.; Donnadiu, B.; Bourissou, D.; Soleilhavoup, M.; Bertrand, G. *J. Am. Chem. Soc.* **2006**, *128*, 14810. (c) Vignolle, J.; Gornitzka, H.; Maron, L.; Schoeller, W. W.; Bourissou, D.; Bertrand, G. *J. Am. Chem. Soc.* **2007**, *129*, 978. (d) Falvello, L. R.; Fernández, S.; Navarro, R.; Urriolabeitia, E. P. *New J. Chem.* **1997**, *21*, 909. (e) Vicente, J.; Chicote, M. T.; Lagunas, M. C. *Inorg. Chem.* **1993**, *32*, 3748. (f) Kawafune, I.; Matsubayashi, G.-E. *Inorg. Chim. Acta* **1983**, *70*, 1. (g) Usón, R.; Forniés, J.; Navarro, R.; Ortega, A. M. *J. Organomet. Chem.* **1987**, *334*, 389. (h) Usón, R.; Laguna, A.; Laguna, M.; Lázaro, I.; Jones, P. G. *Organometallics* **1987**, *6*, 2326. (i) Gimeno, M. C.; Jones, P. G.; Laguna, A.; Villacampa, M. D. *J. Chem. Soc., Dalton Trans.* **1995**, 805. (j) Schmidbaur, H.; Deschler, U.; Milewski-Mahrla, B. *Angew. Chem., Int. Ed. Engl.* **1981**, *20*, 586. (k) Zurawinski, R.; Lepetit, C.; Canac, Y.; Mikolajczyk, M.; Chauvin, R. *Inorg. Chem.* **2009**, *48*, 2147.

Scheme 1. Synthesis of the Ylide–Sulfonium Salt **1** and the Ylide–Sulfide **2**

[Me₂SCHC(O)R], [H₃PCHC(O)CHSMe₂], and their corresponding complexes by means of DFT methods and Bader's analysis of charge density allows the characterization of the ultimate source of the conformational preferences observed, providing further understanding of the chemical behavior of bis–ylides.

Results and Discussion

1. Synthesis of the Organic Precursors. The cationic ylide–sulfonium salt [Ph₃P=CHC(O)CH₂SMe₂]⁺Br⁻ **1** has been prepared previously,¹⁵ but no data concerning its characterization have been given in the original report. Our synthetic method involves the reaction of [Ph₃PCHC(O)CH₂Br]^{16,17} with an excess of SMe₂ (1:40 molar ratio) in MeOH as solvent (Scheme 1) at the reflux temperature. The high polarity of the solvent allows an adequate stabilization of the cationic species, which can be isolated in good yield (74%). Interestingly, the ylide–sulfide [Ph₃P=CHC(O)CH₂SMe] **2** can be prepared following the same procedure but using dry tetrahydrofuran (THF) instead of methanol, this pathway implying the elimination of MeBr during the reaction. The demethylation of sulfonium salts to give the corresponding sulfides is a known process.^{18–20} In our case this process is probably promoted by the presence of the bromide anion acting as a nucleophile.

Compounds **1** and **2** show correct elemental analyses and mass spectra, and **2** behaves as non-electrolyte in acetone solution ($\Lambda_M = 12.7 \Omega^{-1} \text{cm}^2 \text{mol}^{-1}$ for a solution 10^{-4} M).²¹ The IR spectra of **1** and **2** show strong bands at about 1540 cm^{-1} , in keeping with the presence of the ylide–delocalized carbonyl group.^{1j} The ¹H NMR spectra show the expected peaks; therefore, signals at 4.78 (CH₂S), 4.14 (CHP, ²J_{PH} = 21.8 Hz), and 3.16 (SMe₂) ppm are observed for **1**, while the corresponding peaks for **2** appear at 3.17, 4.04 (²J_{PH} = 23 Hz), and 2.13 ppm. The strong shielding of the signals assigned to the CH₂SMe unit with respect to the CH₂SMe₂ moiety is in keeping with the neutral character of the former. Signals observed in the ³¹P-{¹H} and ¹³C-{¹H} NMR spectra are also in good agreement with the structure shown in Scheme 1. The reactivity of **1** and **2** has given quite different results. Because of this reason, they will be treated in different sections.

2. Reactivity of Ylide–Sulfonium Salt 1. Synthesis of Bis–Ylide Complexes. The ylide–sulfonium salt **1** reacts cleanly with NEt₃ and PdCl₂(NCMe)₂ (1:1:1 molar ratio) in MeOH to give the mononuclear derivative *cis*-[PdCl₂[Ph₃PCHC(O)CHSMe₂-*κ*-C,C]] **3**, as represented in Scheme 2. The reaction occurs with deprotonation of the methylene adjacent to the sulfonium unit, formation of the corresponding sulfur ylide, and C,C–chelation of

the resulting bis–ylide to the Pd center. The ammonium salt remains in the alcoholic solution. Complex **3** was very insoluble in the most common deuterated solvents; this prevented its characterization in solution. Because of this fact, it has been transformed into the more soluble acetylacetonate derivative.²² One-pot reaction of **3** with AgClO₄ and Tlacac (1:1:1 molar ratio; acac = acetylacetonate) in CH₂Cl₂ affords **4**, which could be isolated from the insoluble AgCl and TlCl byproducts and properly characterized (Scheme 2). Attempts to isolate the

(11) For selected examples of orthometallated ylides, see: (a) Illingsworth M. L.; Teagle, J. A.; Burmeister, J. L.; Fultz, W. C.; Rheingold, A. L. *Organometallics* **1983**, *2*, 1364. (b) Vicente, J.; Chicote, M. T.; Fernández-Baeza, J. J. *Organomet. Chem.* **1989**, *364*, 407. (c) Onitsuka, K.; Nishii, M.; Matsushima, Y.; Takahashi, S. *Organometallics* **2004**, *23*, 5630. (d) Koch J. L.; Shapley, P. A. *Organometallics* **1999**, *18*, 814. (e) Vicente, J.; Chicote, M. T.; Lagunas, M. C.; Jones, P. G.; Bembenek, E. *Organometallics* **1994**, *13*, 1243. (f) Falvello, L. R.; Fernández, S.; Navarro, R.; Urriolabeitia, E. P. *Inorg. Chem.* **1999**, *38*, 2455. (g) Falvello, L. R.; Fernández, S.; Navarro, R.; Rueda, A.; Urriolabeitia, E. P. *Organometallics* **1998**, *18*, 5887. (h) Falvello, L. R.; Fernández, S.; Larraz, C.; Llusar, R.; Navarro, R.; Urriolabeitia, E. P. *Organometallics* **2001**, *20*, 1424. (i) Gracia, C.; Marco, G.; Navarro, R.; Romero, P.; Soler, T.; Urriolabeitia, E. P. *Organometallics* **2003**, *22*, 4910.

(12) For selected examples of C,C–chelating ylides and bis–ylides, see: (a) Lin, I. J. B.; Shy, H. C.; Liu, C. W.; Liu, L.-K.; Yeh, S.-K. *J. Chem. Soc., Dalton Trans.* **1990**, 2509. (b) Wu, R. F.; Lin, I. J. B.; Lee, G. H.; Cheng, M. C.; Wang, Y. *Organometallics* **1990**, *9*, 126. (c) Basset, J. M.; Mandl, J. R.; Schmidbaur, H. *Chem. Ber.* **1980**, *113*, 1145. (d) Vicente, J.; Chicote, M. T.; Saura-Llamas, I.; López-Muñoz, M. J.; Jones, P. G. *J. Chem. Soc., Dalton Trans.* **1990**, 3683. (e) Schmidbaur, H.; Costa, T.; Milewski-Mahrla, B.; Köhler, F. H.; Tsay, Y.-H.; Krüger, C.; Abart, J.; Wagner, F. E. *Organometallics* **1982**, *1*, 1266. (f) Falvello, L. R.; Margalejo, M. E.; Navarro, R.; Urriolabeitia, E. P. *Inorg. Chim. Acta* **2003**, *347*, 75. (g) Vicente, J.; Chicote, M. T.; Saura-Llamas, I.; Jones, P. G.; Meyer-Bäse, K.; Erdbrügger, C. F. *Organometallics* **1988**, *7*, 997. (h) Falvello, L. R.; Fernández, S.; Navarro, R.; Rueda, A.; Urriolabeitia, E. P. *Inorg. Chem.* **1998**, *37*, 6007. (i) Canac, Y.; Duhaion, C.; Chauvin, R. *Angew. Chem., Int. Ed.* **2007**, *46*, 6313.

(13) For selected structural and DFT studies on conformational preferences on ylides, see: (a) Aitken, R. A.; Karodia, N.; Lightfoot, P. *J. Chem. Soc., Perkin Trans. 2* **2000**, 333. (b) Lledós, A.; Carbó, J. J.; Urriolabeitia, E. P. *Inorg. Chem.* **2001**, *40*, 4913. (c) Lledós, A.; Carbó, J. J.; Navarro, R.; Urriolabeitia, E. P. *Inorg. Chim. Acta* **2004**, *357*, 1444. (d) Lledós, A.; Carbó, J. J.; Navarro, R.; Serrano, E.; Urriolabeitia, E. P. *Inorg. Chem.* **2004**, *43*, 7622. (e) Serrano, E.; Vallés, C.; Carbó, J. J.; Lledós, A.; Soler, T.; Navarro, R.; Urriolabeitia, E. P. *Organometallics* **2006**, *25*, 4653. (f) Serrano, E.; Soler, T.; Navarro, R.; Urriolabeitia, E. P. *J. Mol. Struct.* **2008**, *890*, 57.

(14) For selected examples of C,C–bridging ylides and bis–ylides, see: (a) Schmidbaur, H.; Franke, R. *Angew. Chem., Int. Ed. Engl.* **1973**, *12*, 416. (b) Schmidbaur, H.; Adlkofer, J.; Buchner, W. *Angew. Chem., Int. Ed. Engl.* **1973**, *12*, 415. (c) Dudis, D. S.; Fackler, J. P., Jr. *Inorg. Chem.* **1985**, *24*, 3758. (d) Raptis, R. G.; Porter, L. C.; Emrich, R. J.; Murray, H. H.; Fackler, J. P., Jr. *Inorg. Chem.* **1990**, *29*, 4408. (e) Méndez, L. A.; Jiménez, J.; Cerrada, E.; Mohr, F.; Laguna, M. *J. Am. Chem. Soc.* **2004**, *127*, 852. (f) Vicente, J.; Chicote, M. T.; Saura-Llamas, I.; Jones, P. G. *Organometallics* **1989**, *8*, 767. (g) Trzcinska-Bancroft, B.; Khan, M. N. I.; Fackler, J. P., Jr. *Organometallics* **1988**, *7*, 993. (h) Jandik, P.; Schubert, U.; Schmidbaur, H. *Angew. Chem., Int. Ed. Engl.* **1982**, *21*, 73. (i) Murray, H. H.; Fackler, J. P., Jr.; Mazany, A. M. *Organometallics* **1984**, *3*, 1310. (j) Fackler, J. P., Jr.; Trzcinska-Bancroft, B. *Organometallics* **1985**, *4*, 1891. (k) Usón, R.; Laguna, A.; Laguna, M.; Tartón, M. T.; Jones, P. G. *J. Chem. Soc. Chem. Commun.* **1988**, 740. (l) Usón, R.; Laguna, A.; Laguna, M.; Jiménez, J.; Jones, P. G. *Angew. Chem., Int. Ed. Engl.* **1991**, *30*, 198. (m) King, C.; Heinrich, D. D.; Wang, J. C.; Fackler, J. P., Jr.; Garzon, G. *J. Am. Chem. Soc.* **1989**, *111*, 2300.

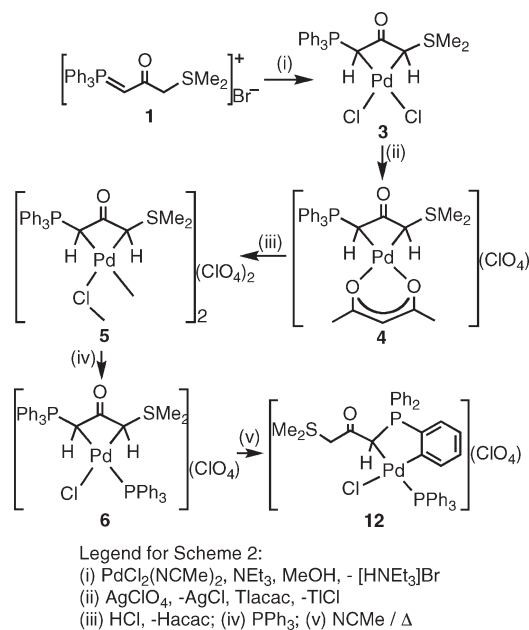
(15) Hercouet, A.; Le Corre, M. *Tetrahedron Lett.* **1976**, *17*, 825. (16) Hudson, R. F.; Chopard, P. A. *J. Org. Chem.* **1963**, *28*, 2446. (17) Hercouet, A.; Le Corre, M. *Tetrahedron* **1977**, *33*, 33–37. (18) Giner, J.; Viñas, C.; Teixidor, F.; Hursthouse, M. B.; Light, M. E. *Dalton Trans.* **2004**, 2059. (19) Nenaidenko, V. G.; Balenkova, E. S. *Russ. J. Org. Chem.* **2003**, *39*, 291.

(20) Clark, J. S. *Nitrogen, Oxygen and Sulfur Ylide Chemistry*; Oxford University Press: New York, 2002.

(21) Geary, W. J. *Coord. Chem. Rev.* **1971**, *7*, 81.

(22) Forniés, J.; Martínez, F.; Navarro, R.; Urriolabeitia, E. P. *J. Organomet. Chem.* **1995**, *495*, 185.

Scheme 2. (i) $\text{PdCl}_2(\text{NCMe})_2$, NEt_3 , MeOH , $-\text{[HNEt}_3\text{]Br}$; (ii) AgClO_4 , $-\text{AgCl}$, Tlaccac , $-\text{TlCl}$; (iii) HCl , $-\text{Hacac}$; (iv) PPh_3 ; (v) NCMe/Δ^a



^a Only the major isomer is shown for **6** and **12**.

expected dinuclear halide bridging **5**, as a result of the reaction of **3** with AgClO_4 (1:1 molar ratio), failed because of the difficulties found in separating **5** from the silver chloride. An alternative procedure to obtain the pure complex **5** is the reaction of **4** with a methanolic solution of HCl (1:1 molar ratio; Scheme 2). The reaction occurs with protonation of the acac group, liberated as acetylacetonate, bonding of the chloride ligand in the vacant coordination sites, and dimerization of the resulting fragments. Complex **5** shows the expected reactivity of a dinuclear halide bridging and, therefore, it reacts with PPh_3 (1:2 molar ratio) giving the mononuclear derivative **6** (Scheme 2). All compounds show correct elemental analyses and mass spectra.

The IR spectra of **3–6** show an intense absorption in the range $1602\text{--}1630\text{ cm}^{-1}$. This band is shifted to higher energies with respect to the ylide–sulfonium salt **1**, and falls in the usual range found for other C,C–chelates.^{12h,13d–13f} Both facts agree with the coordination of the two C atoms. The ^1H NMR spectrum of **4** reveals a static situation in the NMR time scale, which does not change with the temperature, and shows a single set of signals which can be assigned to the presence of the acac ligand and to the $[\text{Ph}_3\text{PCHC}(\text{O})\text{CHSM}_2]$ ligand. The C,C–bonding of the bis–ylide can be inferred from the hybridization change $\text{Csp}^2\text{--Csp}^3$ for the P ylidic moiety,^{1j,1k} which in turn implies: (i) the decrease of the $^2J_{\text{PH}}$ value observed in the signal at 3.63 ppm (4.8 Hz), compared with the homologous in **1** (21.8 Hz); (ii) the low field shift of the phosphorus signal (24.75 ppm) with respect to **1** (15.46 ppm); (iii) the high field shift of the resonances due to the ylidic C atoms (26.22 ppm, CHP; 43.28 ppm, CHS) with respect to their corresponding values in **1**. Moreover, the diastereotopic character of the methyl groups of the SM_2 unit is in good agreement with the presence of the CHS unit. These facts, together with the observation of a single set of signals, means that **4** is

obtained as a unique diastereoisomer. Definitive proof of the stereochemistry of this complex is the presence of an intense NOE at the signal at 4.32 ppm when the resonance at 3.63 ppm is irradiated (and viceversa), implying that both protons are at the same side of the molecular plane and that the bis–ylide is coordinated in the meso form. These results are highly relevant since they point to a coordinating behavior of the sulfur ylides similar to that described previously,^{13f} and also similar to that reported for N- and P-ylides:^{1j,1k} in all cases the meso form is obtained, and it seems logical to propose the existence of conformational preferences in S-ylides, cooperative with those coexisting in P-ylides.

Complex **5** showed a limited solubility in $\text{dms-}d_6$, but it could be characterized in solution as the mixture of two geometric isomers (pseudocis and pseudotrans) derived from the relative arrangement of the ylidic fragments SM_2 and PPh_3 . A pseudocis arrangement is produced when identical fragments are on the same side with respect to the Pd–Pd axis, while if they are on opposite sides, we have a pseudotrans arrangement. This situation is very similar to that observed in related complexes with bis–ylides derived from phosphonium and pyridinium salts.^{13e} Complex **6** shows a set of spectroscopic data consistent with the presence of two geometric isomers (6.7/1 molar ratio), arising from the coordination of the incoming PPh_3 ligand trans to the CHPPh_3 fragment or trans to the CHSM_2 fragment. Since the CHSM_2 group has a lower steric demand compared with the CHPPh_3 moiety, it seems logical to assume that most of the PPh_3 ligand is bonded cis to the former, as represented in Scheme 2, this arrangement being less hindered and more stable. This arrangement has already been observed in mixed bis–ylides derived from pyridinium salts.^{13e} Therefore, the minor isomer would be the most hindered, in which the PPh_3 ligand is cis to the CHPPh_3 unit. The analysis of the NMR spectra of **6** gives proof of these hypotheses. For instance, the signal due to the CHP proton in the major isomer (^1H NMR) appears as a virtual triplet ($^2J_{\text{PH}} \approx ^3J_{\text{PH}}$) while that due to the CHS proton appears as a singlet. Moreover, the signal due to the CHP carbon atom in the major isomer (^{13}C NMR) appears as a doublet of doublets with a large value of the coupling constant $^2J_{\text{PC}}$ (65.8 Hz) while in the minor isomer the observed value is only 9.7 Hz.

In summary, the coordination of the bis–ylide $[\text{Ph}_3\text{PCHC}(\text{O})\text{CHSM}_2]$, derived from deprotonation of **1**, to Pd(II) centers is produced in the meso form. This fact implies that the bonding of stabilized sulfur ylides is also governed by conformational preferences, similarly to other reports dealing with P- and N-ylides. Moreover, the observed behavior shows that the conformational preferences are cooperative and not mutually exclusive.

3. Theoretical Analysis of Conformational Preferences in Sulfur Ylides. We have previously studied the bonding properties and conformational preferences of P-, As- and N-ylides by DFT methods, and Bader's Atoms in Molecules (AIM) theory,²³ showing that the selectivity observed in their coordination modes can be related to the

(23) (a) Bader, R. F. W. *Atoms in Molecules: A Quantum Theory*; Clarendon Press: Oxford, U.K., 1990. (b) Bader, R. F. W. *Chem. Rev.* **1992**, *92*, 893.

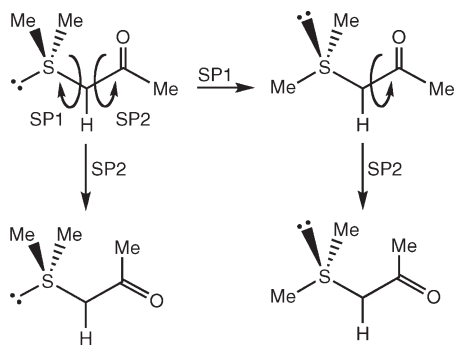


Figure 3. Different rotations on $\text{Me}_2\text{SCHC}(\text{O})\text{Me}$ species **13**.

establishment of different intramolecular interactions.¹³ Thus, we have characterized 1,4- $\text{E}\cdots\text{O}$ electrostatic type interactions between the carbonyl oxygen and the E heteroatoms P and As; and 1,6- $\text{C}-\text{H}\cdots\text{O}=\text{C}$ hydrogen bond interactions in pyridinium ylides. Prompted by these previous results, we have studied the free S-ylide type ligands and their coordinated species using the same methodology.²⁴ Before performing the DFT calculations, we first conducted a detailed search in the Cambridge Crystallographic Data Center.²⁵ The search lead 53 entries for a general structure $[\text{R}_2\text{SC}(\text{R}')\text{C}(\text{O})\text{R}'']$, most of which are doubly stabilized ylides; that is, compounds having two keto and/or ester stabilizing substituents $[\text{R}_2\text{SC}(\text{C}(\text{O})\text{R}')\text{C}(\text{O})\text{R}'']$ (R' and/or $\text{R}'' = \text{alkoxy}$). In all of these structures²⁶ the $\text{C}(\text{O})\text{R}'$ or $\text{C}(\text{O})\text{R}''$ groups are almost coplanar; and at least one of the oxygens points to the S atom, being the dihedral angle $\text{SC}\alpha\text{C}\beta\text{O}$ close to 0° . This means that the free sulfur ylides show a strong preference for the cisoid conformation which is maintained even in the corresponding available coordination complexes.²⁷

Initially, we considered the simple model sulfur ylide $\text{Me}_2\text{SCHC}(\text{O})\text{Me}$ (**13**) to analyze in detail the possible conformational preferences and intramolecular interactions of free ligands. Moreover, because of the characteristics of the SMe_2 group, we have analyzed the conformations resulting from two different rotations: (i) rotation around $\text{S}-\text{C}\alpha$ bond within the observed cisoid conformation (SP1, see Figure 3), and (ii) rotation around the $\text{C}\alpha-\text{C}\beta$ bond to interconvert the cisoid and transoid forms (SP2, see Figure 3). The relaxed energy scan of the rotations around $\text{S}-\text{C}\alpha$ and $\text{C}\alpha-\text{C}\beta$ bonds can be found in the Supporting Information section.

First, the rotation of the SMe_2 group around the $\text{S}-\text{C}\alpha$ bond for compound **13** led to the localization of three different cisoid-type minima **13csym**, **13casym**, and **13canti**, their relative energies being 0.0, +6.5, and +6.5 kcal mol^{-1} , respectively. Figure 4 shows their geometrical structures. In the global minimum **13csym**

the dihedral angles $\text{CSC}\alpha\text{C}\beta$ are 52.1° and -52.7° , showing the two methyl substituents of sulfur in a nearly symmetric arrangement with respect to the ylidic plane formed by the $\text{S}-\text{C}\alpha-\text{C}\beta-\text{O}$ atoms. Both methyl substituents point toward the carbonyl oxygen, whereas the sulfur lone pair should be located opposite to the carbonyl group (see Figure 4). This structure is the most frequently encountered among the 53 X-ray structures mentioned before, regardless if they have one or two stabilizing substituents. Regarding the possible intramolecular interactions, relevant parameters of **13csym** are the $\text{S}\cdots\text{O}$ distance, 3.029 Å, shorter than the sum of the van der Waals radii (3.32 Å)²⁸ and the $\text{CH}\cdots\text{O}$ distances, 2.371 Å and 2.358 Å, typical of weak hydrogen bonds.²⁹ The rotation of about 120° around $\text{S}-\text{C}\alpha$ bond from structure **13csym** led to a new minimum **13casym**, which reflects the arrangement of the SMe_2 group in the X-ray structures of the previously reported coordinated sulfur bis-ylide^{13f} and of **12** (see below). In the new rotamer, one of the methyl groups is in *anti* disposition with respect to the carbonyl group (Figure 4), showing the shortest $\text{S}\cdots\text{O}$ distance (2.791 Å) among all the characterized isomers. Remarkably, the oxygen points to the sulfur atom following the approximation line of a nucleophile to a sulfonium cation; and the resulting arrangement may be considered as an incipient intramolecular nucleophilic attack of the oxygen to the sulfonium group.³⁰ However, although the $\text{S}\cdots\text{O}$ distance in **13casym** is shorter than in **13csym**, the energy of the former is 6.5 kcal mol^{-1} higher. The computed energy barrier associated with the $\text{S}-\text{C}\alpha$ rotation to transform **13csym** into **13casym** amounts to 12.5 kcal mol^{-1} . Finally for rotation around the $\text{S}-\text{C}\alpha$ bond, we found an additional minimum **13canti**, which corresponds to the eclipsed arrangement of the $\text{C}=\text{O}$ bond and the lone pair at the S atom (Figure 4). This structure shows a relatively long $\text{S}\cdots\text{O}$ distance (2.956 Å), which could be explained by the mutual repulsion of the lone pairs at S and O atoms. Interestingly, on going from **13casym** to **13canti** the relaxed scan of the $\text{S}-\text{C}\alpha$ bond rotation led to a very flat potential energy curve, being the two structures degenerate in energy. To explain the energy invariability upon rotation, the increase of the repulsion between the lone pairs of sulfur and oxygen atoms in **13canti** should be balanced by the release of the steric strain in **13casym** (see below). The value of 12.5 kcal mol^{-1} for the rotation barrier indicates that all rotamers could be accessible under experimental conditions through rotation around the $\text{S}-\text{C}\alpha$ bond.

Second, we have analyzed the rotation around $\text{C}\alpha-\text{C}\beta$ bond leading to transoid isomers. Assuming accessible rotation around $\text{S}-\text{C}\alpha$ bond, one should analyze $\text{C}\alpha-\text{C}\beta$ bond rotation from all possible cisoid species. However, we have not found significant differences in geometries and energies for the different paths, and we will base our discussion on the lowest energy species. For S-ylide **13**, calculations show that the cisoid conformation is 9.2 kcal mol^{-1} lower in energy than the transoid one, and that the

(24) Calculations were carried out with the Gaussian03 series of programs using the B3LYP-functional. The basis set for Pd atom was LANL2DZ. For the atoms C, O, P, S, and Cl we used the 6-31G(d) basis set, for the H rest of atoms the 6-31G basis was used. The inclusion of diffuse functions and polarization functions at the H atoms (basis set 6-31 g++(d,p)) was tested and no significant changes in relative energies were observed. See Supporting Information for further details.

(25) Allen, F. H. *Acta Crystallogr. Sect. B* **2002**, *B58*, 380.

(26) Selected references (20) of the CCDC search can be found as Supporting Information

(27) Matsubayashi, G.; Kawafune, I.; Tanaka, T.; Nishigaki, S.; Nakatsu, K. *J. Organomet. Chem.* **1980**, *187*, 113.

(28) Bondi, A. J. *J. Phys. Chem.* **1964**, *68*, 441.

(29) Steiner, T. *Angew. Chem., Int. Ed.* **2002**, *41*, 48.

(30) Briton, D.; Dunitz, J. D. *Helv. Chim. Acta* **1980**, *63*, 1068.

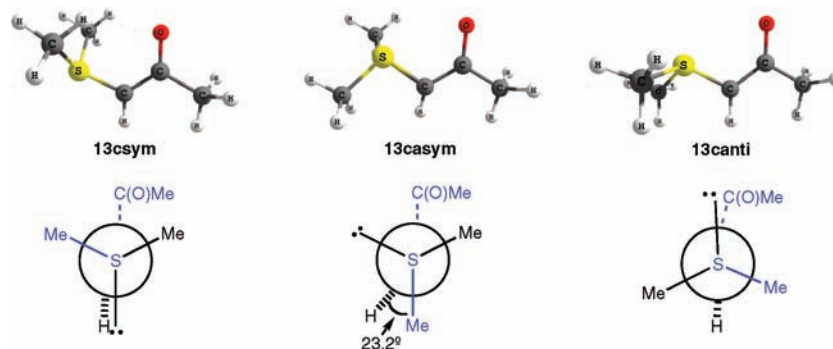


Figure 4. Relevant computed minimum structures for $\text{Me}_2\text{SCHC}(\text{O})\text{Me}$ **13** in cisoid conformation.

rotational barrier is relatively high ($26.2 \text{ kcal mol}^{-1}$). These values agree with the strong cisoid conformational preference found experimentally for ketostabilized sulfur ylides. The results show very similar trends to those observed for model P and N ylides,^{13b,13d} and they could be explained in an analogous way: the cisoid form is favored because of the interaction of the ketonic oxygen with the SMe_2 fragment, while the high rotational barrier reflects the loss of resonance and of intramolecular interaction at the TS.

Once we have computed the energies of the different isomers, the nature of the eventual intramolecular interactions and their influence on the observed conformational preferences remains to be clarified. To assess these questions, we have applied the Bader's atoms in molecules (AIM) theory.²⁴ For the lowest energy conformation **13csym**, we confirmed the existence of two intramolecular $1,6\text{-C-H}\cdots\text{O}$ interactions by the topological analysis of the electron density. These interactions were characterized by the corresponding bond critical points (bcp's) in the electronic charge density $\rho(r)$. On the other hand, no bcp was found between the negatively charged carbonylic oxygen and the positively charged S atom. These results suggest that the methyl substituents on the sulfonium group are able to form hydrogen bonds with the carbonyl oxygen, similarly to pyridinium ylides.^{13d,13e} In addition, on the basis of AIM theory a set of criteria have been proposed to characterize the hydrogen bonds.^{31–33} Following the procedure used for pyridinium ylides,^{13d} we have considered a subset of four criteria that comprise the local topological properties of $\rho(r)$. Table 1 summarizes the results of this analysis and compares them with previous studies. The interactions between the SMe_2 fragment and the carbonyl oxygen fulfill all four criteria: (i) a bond critical point is found between the donor hydrogens and the acceptor oxygen, and the bond path links the two pairs of atoms, (ii) the electron density $\rho(r)$ at the bcp's are low and lie within the typical range of $0.002\text{--}0.040 \text{ au}$, (iii) the Laplacian of the charge density $\nabla^2\rho(r)$ at the bcp's are positive and lie within the typical range of $0.015\text{--}0.150 \text{ au}$, and (iv) there is a positive mutual penetration between hydrogen and the acceptor atom ($\Delta r_{\text{H}} + \Delta r_{\text{A}} > 0$), and the hydrogen atom is more penetrated than the acceptor

Table 1. Topological Properties at the Bond Critical Points of C–H \cdots O Intramolecular Interactions of the S-Ylide **13**; N-Ylide [$\text{H}_5\text{C}_5\text{N}-\text{C}(\text{H})\text{C}(\text{O})-\text{CH}_3$]; and MDAE.^a

	$d(\text{\AA})$	$\rho(r)^c$	$\nabla^2\rho(r)^c$	Δr_{H}^d	Δr_{A}^d	$\Delta r_{\text{H}} + \Delta r_{\text{A}}^d$	$\Delta_{\text{geo+el+lap}}^e$
N-ylide ^b	1.957	0.030	0.099	0.463	0.298	0.761	0.106
13csym	2.358	0.014	0.047	0.248	0.108	0.356	0.073
	2.371	0.013	0.045	0.242	0.098	0.340	0.077
MDAE ^b	2.337	0.014	0.048	0.248	0.137	0.385	0.062

^a 1-Methoxy-2-(dimethylamino)ethane, MDAE. ^b Values taken from ref 11. ^c Electron charge density, $\rho(r)$, and Laplacian, $\nabla^2\rho(r)$, in au. ^d Penetration of the hydrogen atom, Δr_{H} , penetration of the acceptor atom Δr_{A} , mutual penetration $\Delta r_{\text{H}} + \Delta r_{\text{A}}$, in \AA . ^e Modified Grabowski's complex parameter $\Delta_{\text{geo+el+lap}}$ (ref 35).

atom ($\Delta r_{\text{H}} > \Delta r_{\text{A}}$) (see Table 1).³⁴ Thus, the $1,6\text{-C-H}\cdots\text{O}$ interactions characterized for S-ylides can be unambiguously assigned to true hydrogen bonds.

To estimate the strength of the intramolecular hydrogen bonds, we have used a procedure based also on AIM properties. Grabowski has proposed a complex parameter ($\Delta_{\text{geo+el+lap}}$) based on structural data and topological parameters for describing hydrogen bond strength.³⁵ We have already used the Grabowski's parameter for evaluating intramolecular hydrogen bond strength in pyridinium ylides.^{13d} Here, we compare the computed $\Delta_{\text{geo+el+lap}}$ values for S-ylides with those of previous study (Table 1), assuming that AIM results are system independent.²⁴ For N-ylide [$\text{H}_5\text{C}_5\text{N}-\text{C}(\text{H})-\text{C}(\text{O})-\text{CH}_3$] and the reference compound 1-methoxy-2-(dimethylamino)ethane (MDAE)³⁶ the calculated $\Delta_{\text{geo+el+lap}}$ parameters were 0.106 and 0.062, respectively, whereas the estimated intramolecular interaction energies were 10 and 2 kcal mol^{-1} , respectively. In the case of S-ylide **13csym**, the $\Delta_{\text{geo+el+lap}}$ values (0.073 and 0.077) are closer to the MDAE values than to the N-ylide ones, i.e., closer to weak than to moderate hydrogen bonding. However, for **13csym**, $\Delta_{\text{geo+el+lap}}$ values are somewhat larger than for MDAE, suggesting that the intramolecular interaction could be also somewhat stronger, about 3–4 kcal mol^{-1} for each hydrogen bond. Obviously, this is a rough approximation, but is still meaningful for our purposes. Thus, most of the energy difference between the cisoid structure **13csym** and the transoid structure (9.2 kcal mol^{-1}) could be explained from the formation of two intramolecular hydrogen bonds (6–8 kcal mol^{-1}).

Finally, we analyze the possible intramolecular interactions in cisoid rotamer **13casym**, in which the SMe_2 group

(31) Popelier, P. L. A. *J. Phys. Chem. A* **1998**, *102*, 1873.

(32) Koch, U.; Popelier, P. L. A. *J. Phys. Chem. A* **1995**, *99*, 9747.

(33) Pacios, L. F.; Gómez, P. C. *J. Comput. Chem.* **2001**, *22*, 702.

(34) The penetration was evaluated as the difference between the nonbonded van der Waals type radius and the bonding radius defined as the distance between the corresponding bcp.

(35) Grabowski, S. J. *J. Phys. Chem. A* **2001**, *105*, 10739.

(36) Matura, H.; Yoshida, H.; Hieda, M.; Yamanaka, S.; Harada, T.; Shin-Ya, K.; Ohmo, K. *J. Am. Chem. Soc.* **2003**, *125*, 13910.

has the same arrangement as in the X-ray determined coordination complexes. This structure is $6.5 \text{ kcal mol}^{-1}$ higher in energy than the global minimum **13csym**, but still $2.7 \text{ kcal mol}^{-1}$ more stable than the transoid isomer. The calculated $\text{S}\cdots\text{O}$ distance (2.791 \AA) is the shortest among the series of isomers, whereas the closest $\text{CH}\cdots\text{O}$ distance is relatively long (2.977 \AA), precluding hydrogen bonding. Thus, it is reasonable to think that in **13casym** there is some kind of weak intramolecular interaction between the carbonylic oxygen and the sulfur atoms responsible for its stabilization with respect to the transoid isomer. Nevertheless, and in spite of an extensive research, it was not possible to localize any bcp between the oxygen and the sulfur atoms of structure **13casym**. This is quite surprising because $1,5\text{-S}\cdots\text{O}$ intramolecular interactions on α,α' -bithiophene derivatives were characterized by Bader's analysis at interatomic distances ranging from 2.88 to 2.91 \AA ,^{37,38} still longer than that for **13casym** (2.791 \AA). To back up our methodology and to allow direct comparison with S-ylides, we have performed Bader's AIM analysis on the $2,2'$ -bithiophene containing an OMe substituent in β position at the same computational level of this work. The computed $\text{S}\cdots\text{O}$ distance is 2.909 \AA , showing an excellent agreement with the previous reported distance (2.906 \AA).³⁸ Contrary to S-ylides, we have located a bcp between the oxygen and sulfur atoms and the corresponding rcp for bithiophene structure, evidencing the intramolecular interaction. Figure 5 shows the contour maps of the charge density $\rho(r)$ for the S-ylide **13casym** (Figure 5a) and the calculated bithiophene structure (Figure 5b). To understand the observed differences on charge density distribution patterns between $1,4\text{-S}\cdots\text{O}$ and $1,5\text{-S}\cdots\text{O}$ contacts, one should consider the spatial arrangement of the charge density in the determination of non-bonded intramolecular interactions.³¹ The calculated value of the $\text{C}-\text{O}\cdots\text{S}$ angle in the S-ylide **13casym** is significantly smaller (68.6°) than that calculated for bithiophene structure (88.0°). Thus, in the case of bithiophene, the lone pair of the oxygen atom is better oriented for establishing an electrostatic interaction with the positively charged S atom, explaining why $1,5\text{-S}\cdots\text{O}$ intramolecular interactions could be characterized through Bader's AIM theory.

Taking a closer look to the calculated geometry of **13casym**, we could observe another noteworthy structural feature. The $\text{S}-\text{C}_\alpha-\text{C}_\beta$ bond angle is 112.4° , notably smaller than the expected 120° , and than that found in the transoid structure (123.8°), where no $\text{S}\cdots\text{O}$ interaction is possible. The bond angle distortion suggests the formation of an interaction between the S and O atoms to counterbalance the increase of steric stress. In fact, we observed an analogous phenomenon for P-ylides, in which the $1,4\text{-P}\cdots\text{O}$ interaction was characterized at a $\text{P}-\text{C}_\alpha-\text{C}_\beta$ bond angle value of 100.9° . Thus, we have analyzed in more detail the energy curve associated with $\text{SC}_\alpha\text{C}_\beta$ angle distortion in the cisoid rotamer **13casym**, and compared it with that for transoid isomer (Figure 6). For the transoid isomer, where no stabilizing intramolecular interactions

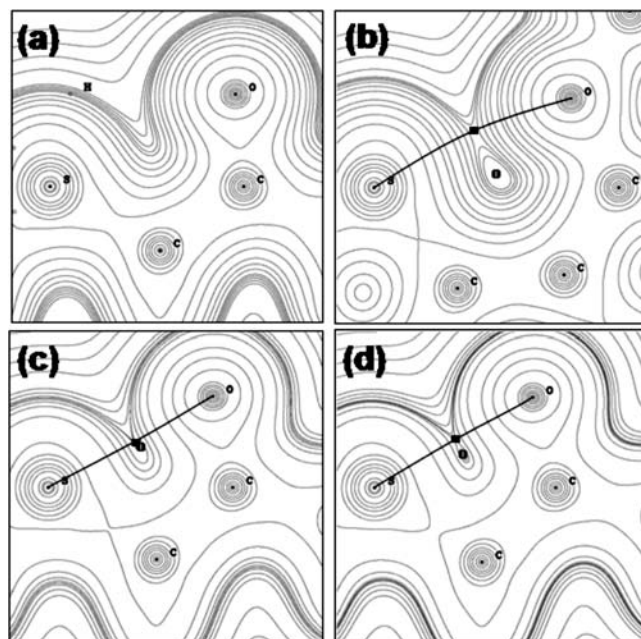


Figure 5. Contour maps of electron charge density $\rho(r)$ at the $\text{S}-\text{O}=\text{C}$ plane for **13casym** (a), the monosubstituted α,α' -bithiophene (b), and **13casym** at distorted $\text{S}-\text{C}_\alpha-\text{C}_\beta$ bond angles of 103° (c) and 100° (d). The solid squares represent the bcp's and the circles the rcp's.

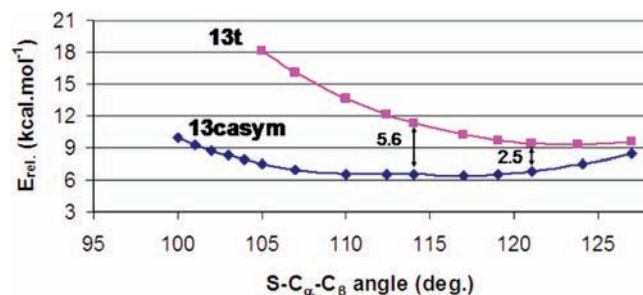


Figure 6. Potential energy curves of the $\text{S}-\text{C}_\alpha-\text{C}_\beta$ bond angle distortion for cisoid **13casym** and transoid **13t** compounds. Relative energies in kcal mol^{-1} respect to the lowest energy rotamer **13csym**.

are present, the energy rises continuously as we distort the $\text{SC}_\alpha\text{C}_\beta$ angle from its equilibrium value 123.8° . In the case of the cisoid structure **13casym**, the energy curve is shifted down in energy. The energy difference between the distortion energy curves of transoid and cisoid isomers can be attributed to the formation of the stabilizing nonbonding interactions between the SMe_2 fragment and the carbonylic oxygen in the cisoid structure. Note also that starting at a $\text{SC}_\alpha\text{C}_\beta$ value of 124° , the smaller the $\text{SC}_\alpha\text{C}_\beta$ value is the larger the energy differences between the distorted cisoid and transoid structures because of the reinforcement of the stabilizing intramolecular interactions upon shortening of $\text{S}\cdots\text{O}$ distance. In **13casym**, the balance between distortion and intramolecular interactions leads to a displacement of the minimum to narrower $\text{SC}_\alpha\text{C}_\beta$ angle (112.4°), and to a very flat potential energy surface, in which the variation of $\text{SC}_\alpha\text{C}_\beta$ angle from 101° to 121° has an energy cost of only $0.2 \text{ kcal mol}^{-1}$.

Interestingly, we could locate bcp's between the S and O atoms at narrow $\text{SC}_\alpha\text{C}_\beta$ angle values ranging from 100° to 103° ($\text{S}\cdots\text{O}$ distance 2.46 – 2.53 \AA) for **13casym**. On going from $\text{SC}_\alpha\text{C}_\beta = 100^\circ$ to 103° the distance between the

(37) Réthoré, C.; Madalan, A.; Fourmigué, M.; Canadell, E.; Lopes, E. B.; Almeida, M.; Clérac, R.; Avarvari, N. *New J. Chem.* **2007**, *31*, 1468.

(38) Raos, G.; Famulari, A.; Meille, S.; Gallazzi, M. C.; Allegra, G. *J. Phys. Chem. A* **2004**, *108*, 691.

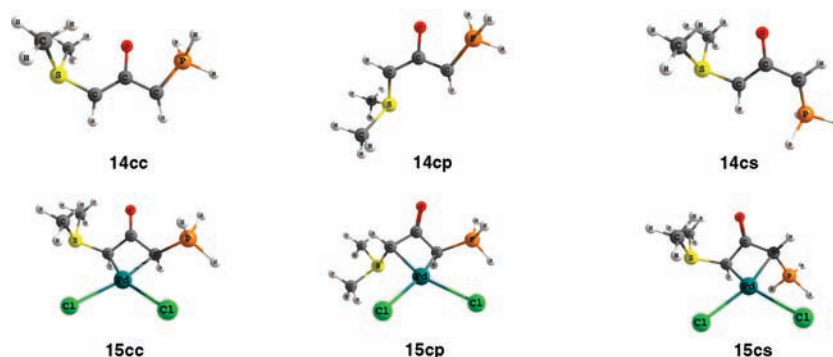


Figure 7. Computed structures for mixed bis-ylide $\text{Me}_2\text{SCHC}(\text{O})\text{CHPH}_3$ and its corresponding complexes.

bcp and the corresponding rcp diminishes from 0.24 to 0.07 Å. This means that, in the direction perpendicular to the S–O bond path, a maximum of charge density corresponding to the bcp becomes very close to a minimum corresponding to the rcp, and finally, both critical points collapse (Figure 5: $d \rightarrow c \rightarrow a$). Therefore, for $\text{SC}_\alpha\text{C}_\beta$ angles larger than 103° it was not possible to characterize the $1,4\text{-S}\cdots\text{O}$ interactions by Bader's AIM theory in cisoid isomers. Note that during the last years the role of bond paths and bcp's of $\rho(r)$ as a direct interpretation of chemical interactions has been a matter of debate in the chemical community.³⁹ These arguments, in conjunction with the geometric and energetic evidence stated above, indicate that in cisoid isomers a $1,4\text{-S}\cdots\text{O}$ type interaction can also take place, despite the fact that it is not being manifested by a bcp. Moreover, we can estimate the $\text{S}\cdots\text{O}$ interaction strength through comparison of distortion energy curves in Figure 6. For an $\text{SC}_\alpha\text{C}_\beta$ angle 112.4° (value in **13casym**), the estimated stabilizing $\text{S}\cdots\text{O}$ interaction energy is about $5.6 \text{ kcal mol}^{-1}$, balancing the energy required for an $\text{SC}_\alpha\text{C}_\beta$ angle distortion (estimated in about $2.8 \text{ kcal mol}^{-1}$ from the **13t** distortion curve) and explaining the computed energetic preference of **13casym** with respect to transoid isomers. Following the same procedure for the $\text{SC}_\alpha\text{C}_\beta$ angle of 121° (value in **13csym**), the distortion-interaction balance results in an overall stabilization of about $2.5 \text{ kcal mol}^{-1}$, which can be attributed exclusively to a weak stabilizing $\text{S}\cdots\text{O}$ contact since the closest $\text{CH}\cdots\text{O}$ distance is 4.42 Å. Note also that if we add the contribution of this weak $\text{S}\cdots\text{O}$ contact to the value estimated for the formation of two weak hydrogen bonds ($6\text{--}8 \text{ kcal mol}^{-1}$), then we better explain the energy difference between **13csym** and the transoid isomer ($9.2 \text{ kcal mol}^{-1}$).

In summary, ketostabilized sulfur ylides show conformational preferences similar to those reported for N- and P-ylides, which favor the cisoid form. Theoretical analysis allowed identifying and evaluating two types of weak stabilizing non-bonded intramolecular interactions between the SMe_2 fragment and carbonyl oxygen: the $1,6\text{-CH}\cdots\text{O}$ hydrogen bonds and $1,4\text{-S}\cdots\text{O}$ interaction, which are the ultimate reason of the conformational preferences. Moreover, both types of interactions can occur simultaneously in a cooperative way.

4. Theoretical Analysis of Conformational Preferences and Coordination Properties of Mixed Bis-Ylides of Phosphorus and Sulfur.

Once we have analyzed in detail the origin of conformational preferences on free S-ylides, the next step in our discussion is centered on the mixed P–S bis-ylide ligands [$\text{Me}_2\text{SCHC}(\text{O})\text{CHPH}_3$] (**14**) and on their corresponding palladium complexes [$(\text{Me}_2\text{SCHC}(\text{O})\text{CHPH}_3)_2\text{PdCl}_2$] **15**. Figure 7 shows the computed structures, and geometric parameters are provided in the Supporting Information, Table S2. As expected the cisoid–cisoid conformation of free ligand **14cc** is the most stable rearrangement, being the P-cisoid-S-transoid (**14cp**) and the P-transoid-S-cisoid (**14cs**) structures less stable by 8.1 and $10.3 \text{ kcal mol}^{-1}$, respectively. We could not find a minimum for the transoid-transoid isomer since all the attempts to optimize such geometry ended in the **14cs** structure. The most stable isomer **14cc** is rigorously planar, and it shows the presence of a $1,4\text{-P}\cdots\text{O}$ interaction ($d(\text{P}\cdots\text{O}) = 2.381 \text{ Å}$, $a(\text{PC}_\alpha\text{C}_\beta) = 103.7^\circ$, and bcp between the P and O atoms).^{13b,13c,13e} The sulfonium half in **14cc** shows the same types of interactions between the SMe_2 fragment and the carbonyl oxygen ($d(\text{H}\cdots\text{O}) = 2.369 \text{ Å}$, $d(\text{S}\cdots\text{O}) = 3.030 \text{ Å}$, and bcp's between the H's and O atoms) as in S-ylide **13sym**. On going from **14cc** to **14cp**, two $1,6\text{-C}\cdots\text{O}=\text{C}$ hydrogen bonds and one $1,4\text{-S}\cdots\text{O}$ weak-type intramolecular interactions disappear explaining the energy raising of $8.1 \text{ kcal mol}^{-1}$. This provides further evidence of the stabilizing interaction between SMe_2 fragment and carbonyl oxygen. Moreover, it shows that the intramolecular interactions characterized in the two halves of the mixed P–S bis-ylides are cooperative leading to the conformational preference of the cisoid–cisoid isomer.

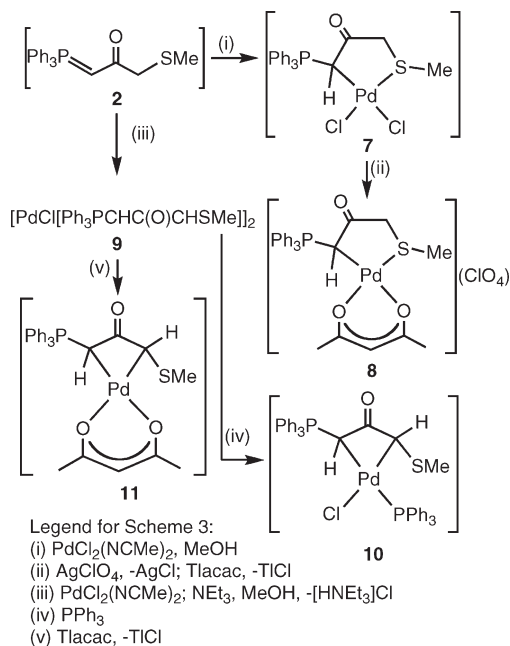
The coordination of ligands **14cc**, **14cp**, and **14cs** to the PdCl_2 group results in the formation of the C,C-chelates **15cc**, **15cp**, and **15cs**, respectively (Figure 7). Not surprisingly, the meso form **15cc** is the most stable isomer, in very good agreement with the experimental data (synthesis of complexes **3–6**), being the d,l forms **15cp** and **15cs** destabilized by 6.7 and $6.6 \text{ kcal mol}^{-1}$, respectively. The destabilization of the d,l forms with respect to the meso form is smaller than in the free ligands probably because of the elongation of intramolecular contacts upon coordination, this fact promoting an attenuation of the interactions. Anyway, there is a clear transfer of the conformational preferences from the free ligand to the complex, and it is possible to explain the observed stereoselectivity of the

(39) See for example: (a) Grimme, S.; Mück-Lichtenfeld, C.; Erker, G.; Kehr, G.; Wang, H.; Beckers, H.; Willner, H. *Angew. Chem., Int. Ed.* **2009**, *48*, 2592. (b) Cerpa, E.; Krapp, A.; Vela, A.; Merino, G. *Chem.—Eur. J.* **2008**, *14*, 10232 and references therein.

bonding of the bis-ylides from their structure in free form. An additional question to be addressed is the orientation of the SMe_2 groups with respect to the carbonyl group. The X-ray structures of the previously reported coordinated sulfur bis-ylide bridging two Pd atoms^{13f} and that reported in this work (**12**, see below) showed an asymmetric arrangement of methyl substituents. On the other hand, in the calculated lowest energy rotamer of complex **15cc**, the methyl groups are nearly symmetric forming two hydrogen bonds. Nevertheless, the rotamer with the asymmetric (X-ray-like) orientation of sulfonium unit (**15cc'**) is only 1.1 kcal mol⁻¹ higher in energy. Therefore, and assuming a low S-C_α rotational barrier, both orientations of the sulfonium fragment should be energetically accessible, and subtle effects should modulate their energetic balance. This would explain why previously reported X-ray structures,^{13f} or those in this work, show an asymmetric orientation of the sulfonium moiety.

5. Reactivity of Ylide-Sulfide 2. Synthesis of Ylide-Methanide Complexes. The ylide-sulfide $[\text{Ph}_3\text{PCHC}(\text{O})\text{CH}_2\text{SMe}]$ **2** possess at least two strong donor atoms, the sulfur and the ylidic carbon. Then it is not surprising that the reaction of **2** with $[\text{PdCl}_2(\text{NCMe})_2]$ (1:1 molar ratio) occurs with displacement of both nitrile ligands and C,S-chelation of **2**, giving *cis*- $[\text{PdCl}_2[\text{Ph}_3\text{PCHC}(\text{O})\text{CH}_2\text{SMe-}\kappa\text{-C,S}]]$ **7**. Complex **7** reacts with AgClO_4 and Tlacac (1:1:1 molar ratio) to give $[\text{Pd}(\text{acac-O,O}')[\text{Ph}_3\text{PCHC}(\text{O})\text{CH}_2\text{SMe-}\kappa\text{-C,S}]]\text{ClO}_4$ **8** (Scheme 3). The C-bonding of the ylidic carbon in **7** and **8** is inferred from the comparison of their IR and NMR parameters with those of **2**, in the same way than reported for **1-6**: the increase of the carbonyl stretch (IR), the decrease of the values of the coupling constants $^2J_{\text{PH}}$ and $^1J_{\text{PC}}$, the low field shift of the ^{31}P signal, and the shielding of the ylidic carbon signal in the ^{13}C NMR spectra. The low field shift of the methyl resonances in the NMR spectra (SCH_3 in ^1H and SCH_3 in ^{13}C) strongly suggest the S-bonding. In addition, the S-coordination of **2** introduces a second stereogenic center in **7** and **8**, which are obtained as mixtures of diastereoisomers (see Supporting Information). Both the C bonding of the ylide, as well as the S bonding of the sulfide, should be configurationally stable in the NMR time scale, as it seems clear from the shape of the signals. In these conditions, the 2D NOESY spectrum of **8** allows the determination of the stereochemistry of each diastereoisomer. Obviously, each diastereoisomer is obtained as the racemic mixture, and the product, as a whole, is not optically active. For the minor isomer, a clear NOE between the ylidic proton (5.99 ppm) and the methyl protons of the SMe group (2.79 ppm) is observed, showing that both units are on the same side of the molecular plane (Supporting Information). A strong NOE between the ylidic proton (5.99 ppm) and one of the methylenic protons (4.23 ppm) is also observed. The configurations shown in the Supporting Information for the minor isomer of **8** ($R_{\text{C}}S_{\text{S}}/S_{\text{C}}R_{\text{S}}$) agree with these observations. In addition, the major isomer shows a NOE effect between the ylidic proton (5.60 ppm) and one of the methylenic protons (4.37 ppm) and an additional NOE between the other methylenic proton (2.49 ppm) and the methyl protons (2.41 ppm), showing that the former and the latter are on different sides of the molecular plane.

Scheme 3. (i) $\text{PdCl}_2(\text{NCMe})_2$, MeOH; (ii) AgClO_4 , $-\text{AgCl}$; Tlacac, $-\text{TlCl}$; (iii) $\text{PdCl}_2(\text{NCMe})_2$; NEt_3 , MeOH, $-\text{[HN(Et)}_3\text{]Cl}$; (iv) PPh_3 ; (v) Tlacac, $-\text{TlCl}$



More interestingly, **2** reacts with $\text{PdCl}_2(\text{NCMe})_2$ in presence of NEt_3 (1:1:1 molar ratio) to give **9**, a complex of stoichiometry $[\text{PdCl}[\text{Ph}_3\text{PCHC}(\text{O})\text{CHSMe}]]$ (see Scheme 3). The reaction occurs through deprotonation of the methylene unit in **2**, which results in the synthesis of the ylide-methanide anion $[\text{Ph}_3\text{PCHC}(\text{O})\text{CHSMe}]^-$. The dimeric nature of **9** was inferred from its MALDI+ spectrum, which shows a strong peak at 975 amu, with the correct position and isotopic distribution for the stoichiometry $[\text{Pd}_2[\text{Ph}_3\text{PCHC}(\text{O})\text{CHSMe}]_2\text{Cl}]^+$. Attempts to determine the molecular weight in CHCl_3 solution gave erratic results, probably because of its low solubility in this solvent. While the C,C-bonding of the ylide-methanide seems clear from the IR data (strong absorption at 1593 cm^{-1}), the nature of the bridging ligands can not be determined unambiguously from the spectroscopic parameters. The chemical shift of the SMe protons in **9** (2.44 ppm) is shifted downfield with respect to **2** (2.13 ppm) and falls in the same region as those found for S-bonded derivatives as **7** (2.42 and 2.50 ppm) or **8** (2.41 ppm), suggesting S-bonding. On the other hand, the IR spectrum of **9** shows absorptions in the low energy region at 251, 243, 239, and 237 cm^{-1} , this observation being in agreement with either a bridging chloride structure^{40a} or a terminal Pd-Cl bond trans to an atom with large trans influence,^{40b} as it could be the methanide carbon. In spite of this ambiguity, and according with its dimeric nature, $[\text{PdCl}[\text{Ph}_3\text{PCHC}(\text{O})\text{CHSMe}]_2$ **9** reacts with strong donors and with chelating ligands, allowing a proper characterization of the bonding mode of the ylide-methanide ligand.

The reaction of a suspension of **9** with PPh_3 (1:2 molar ratio) gives the mononuclear $[\text{Pd}(\text{Cl})(\text{PPh}_3)[\text{Ph}_3\text{PCHC}(\text{O})\text{CHSMe-}\kappa\text{-C,C}]]$ **10**, while treatment of **9** with Tlacac

(40) (a) Usón, R.; Forniés, J.; Martínez, F.; Tomas, M.; Reoyo, I. *Organometallics* **1983**, *2*, 1386. (b) Nonoyama, M. *Trans. Met. Chem.* **1987**, *12*, 1-3.

gives $[\text{Pd}(\text{acac}-\text{O},\text{O}')][\text{Ph}_3\text{PCHC}(\text{O})\text{CHSM}e-\kappa-\text{C},\text{C}]$ **11** (Scheme 3). The structure of **10** has been determined by X-ray diffraction methods, and shows some amazing features. A drawing of complex **10** is shown in Figure 8, selected bond distances (Å) and angles (deg) are collected in Table 2, and the most relevant parameters concerning data collection and structure solutions and refinement are given in the Supporting Information, Table S1. The Pd atom is located in a distorted square-planar environment, surrounded by the ylidic carbon C(37), the methanide carbon C(39), the chlorine atom Cl(1), and the P atom of the phosphine ligand P(1). This fact confirms the chelating bonding mode of the ylide-methanide ligand, the nonbonding of the sulfur atom, and the cis arrangement of the bulky phosphine and the CH(SMe) fragment. The four membered ring comprising the chelating ylide-methanide $[\text{C}37\text{P}1\text{C}39\text{O}1]$ is the main one responsible of the distortion of the square-planar environment. The most noteworthy features are the cisoid arrangement of the C(37)–P(2) and C(38)–O(1) bonds, reflected in the distance P(2)–O(1) = 3.11 Å and in the dihedral angle O(1)–C(38)–C(37)–P(2) = -3.2° , and the alterned disposition of the C(38)–O(1) and C(39)–S(1) bonds. That is, the ylidic moiety involving the phosphorus atom behaves as expected, adopting the same distribution of bonds as observed previously, while the methanide unit coordinates showing the opposite conformation to that shown by sulfur ylides. The absolute configurations of the bonded carbons shown in Figure 8 are $R_{\text{C}39}$ and $R_{\text{C}37}$, although both enantiomers are present in the crystal which, as a whole, is racemic ($R_{\text{C}}R_{\text{C}}/S_{\text{C}}S_{\text{C}}$). Therefore, the simple change from the sulfur ylide to the sulfide reverses the selectivity of the coordination and, instead of the expected cisoid form, the transoid conformation is obtained.

The Pd(1)–C(37) bond distance [2.181(3) Å] falls in the usual range of distances found for C-bonded ylides trans to a phosphine ligand,^{11g} while the Pd(1)–C(39) bond distance [2.086(3) Å] is slightly longer than those found in palladium complexes with related methanide-sulfide ligands [ranging from 2.035(3) to 2.044(4) Å].⁴¹ Probably the difference arises from the different substituents of the sulfide and from the different bonding mode. The Pd–Cl and Pd–P bond distances (Table 2) are typical for this type of bonds.⁴² Concerning the ylide-methanide skeleton, the bond distances C(38)–C(37) [1.489(5) Å] and C(38)–C(39) [1.491(4) Å] reflect charge delocalization and are identical, within experimental error, to those found in bonded bis-ylides.^{12h,13e,13f} This fact is also reflected in the C(38)–O(1) bond distance [1.237(4) Å]. On the other hand, the S–C and P–C bond distances are also similar to those found in related complexes,^{12h,13e,13f,41} while other internal parameters are as expected.

The interpretation of the spectroscopic parameters of **10** (IR and NMR) agrees with its crystal structure and suggests a static behavior in solution. The IR shows a strong band at 1590 cm^{-1} , according with the formation

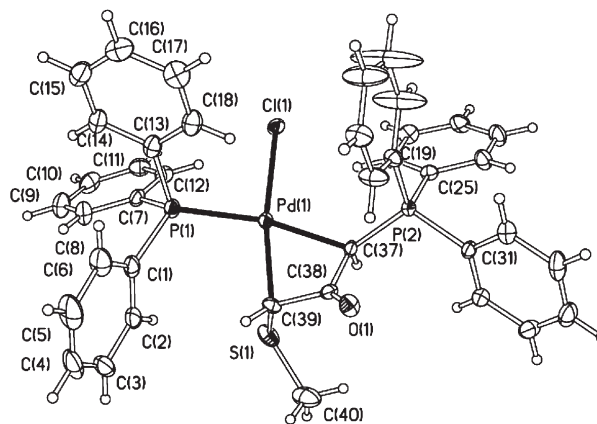


Figure 8. Thermal ellipsoid plot of complex **10**. Non-hydrogen atoms are drawn at the 50% probability level.

of a C,C-chelating four membered ring. The C-bonding of the ylide can be inferred from the NMR data using the same key features than in the preceding section: (i) decrease of the values of the $^2J_{\text{PH}}$ and $^1J_{\text{PC}}$ coupling constants with respect to **2**; (ii) low field shift of the ^{31}P signal; and (iii) high field shift of the signal of the ^{13}C ylidic carbon. The trans coordination of the PPh_3 ligand with respect to the phosphorus ylide moiety is also evident from the shape and coupling constant values of the CHP signals in the ^1H ($^3J_{\text{PH}} = 7.0\text{ Hz}$) and ^{13}C ($^2J_{\text{PC}} = 48.1\text{ Hz}$) NMR spectra. The nonbonding of the SMe group in **10** can also be detected in the ^1H NMR spectrum, since the chemical shift of the SMe protons is slightly shifted to high field in **10** (1.96 ppm) with respect to **2** (2.13 ppm), while a clear low field shift has been observed when the SMe group is bonded, for instance, in **8** (2.41 or 2.79 ppm). Unfortunately, NOESY 1D experiments are not informative in this case, since irradiation of the CHP or CHS protons produce NOE effects only in their respective neighboring protons (PPh_3 and SMe), but the absence of NOE between the CHP and CHS nuclei can not be considered a proof of their relative transoid disposition.⁴³ The comparison of the IR and NMR data of **11** with those reported for **10** (see Supporting Information) allows to propose a chelating structure with the nonbonded SMe fragment, as represented in Scheme 3.

In summary, the ylide-sulfide ligand $[\text{Ph}_3\text{PCHC}(\text{O})\text{CH}_2\text{SMe}]$ coordinates to the Pd as a chelate $\kappa^2\text{-C,S}$, and can be easily deprotonated at the methylene group to give the ylide-methanide anion $[\text{Ph}_3\text{PCHC}(\text{O})\text{CHSM}e]^-$. This anion can behave as chelate $\kappa^2\text{-C,C}$ ligand, and shows also strong conformational preferences but opposite to those found on bis-ylides: while the latter favor the RS/SR configurations (meso form), the former gives exclusively the RR/SS configurations (d,l pair). We have attempted a similar theoretical analysis, searching for the presence of conformational preferences, but the situation is less clear in the anionic species than in the neutral ones. It seems sensible to assume that the interactions involving the SMe fragment should be weaker in $[\text{H}_3\text{PCHC}(\text{O})\text{CHSM}e]^-$ than in $[\text{H}_3\text{PCHC}(\text{O})\text{CHSM}e_2]$ because of the change of the net charge: the protons of the $\text{CHSM}e$ are

(41) (a) Basato, M.; Bertani, C.; Zecca, M.; Grassi, A.; Valle, G. *J. Organomet. Chem.* **1999**, 575, 163. (b) Basato, M.; Grassi, A.; Valle, G. *Organometallics* **1995**, 14, 4439.

(42) Orpen, A. G.; Brammer, L.; Allen, F. H.; Kennard, O.; Watson, D. G.; Taylor, R. *J. Chem. Soc., Dalton Trans.* **1989**, S1.

(43) Claridge, T. D. W. *High Resolution NMR Techniques in Organic Chemistry*, 2nd ed.; Elsevier: Oxford, U.K., 2009.

Table 2. Selected Bond Distances (Å) and Angles (deg) for **10**

Pd(1)–C(39)	2.086(3)	Pd(1)–C(37)	2.181(3)
Pd(1)–P(1)	2.297(9)	Pd(1)–Cl(1)	2.399(8)
C(38)–O(1)	1.237(4)	C(38)–C(37)	1.489(5)
C(38)–C(39)	1.491(4)	C(39)–S(1)	1.795(3)
S(1)–C(40)	1.820(5)	P(2)–C(37)	1.773(3)
C(37)–Pd(1)–C(39)	68.33(13)	C(37)–Pd(1)–Cl(1)	101.35(9)
C(39)–Pd(1)–Cl(1)	169.36(10)	C(37)–Pd(1)–P(1)	167.60(9)
C(39)–Pd(1)–P(1)	99.73(10)	P(1)–Pd(1)–Cl(1)	90.72(3)
O(1)–C(38)–C(39)	107.2(3)	O(1)–C(38)–C(37)	126.4(3)
C(39)–C(38)–C(37)	107.2(3)	C(38)–C(39)–S(1)	116.2(2)
C(38)–C(39)–Pd(1)	83.88(18)	S(1)–C(39)–Pd(1)	107.22(16)
C(39)–S(1)–C(40)	100.3(2)	P(2)–C(37)–C(38)	118.1(2)
P(2)–C(37)–Pd(1)	123.13(17)		

less positive, the own S atom also, and there is an additional lone pair over the S atom interacting with the O atom. Probably, all these facts militate against the establishment of conformational preferences on the sulfur side. It is interesting to note that those in the phosphorus side are maintained because of the cationic character of the CHPR₃ group. Clearly, this area needs further development.

6. Orthometalation of Bis–Ylides. The enormous importance of the CH bond activation processes nowadays is doubtless because of their implications in the functionalization of organic substrates.^{44,45} We have studied the selective orthometalation of iminophosphoranes and ylides, and related species,^{46–52} and we have also reported that dinuclear complexes containing chelating bis–ylides are adequate precursors for the synthesis of orthopalladated complexes through CH activation (Figure 1).^{1j,1k,11g,13e} These syntheses have been achieved by either thermal induction or ligand addition, the steric effects being the driving force in the latter cases. We have attempted the orthopalladation of mixed phosphorus–sulfur bis–ylides by thermal treatment of dimer **5** (NCMe, reflux, 24 h), but no reaction was observed since the starting compound was recovered. However, refluxing of **6** in NCMe for 24 h affords cleanly **12** (Scheme 2) as a mixture of two geometric isomers (6.7/1 molar ratio). For complex **5**, the pattern of reactivity is similar to that found with mixed phosphonium–pyridinium ylides,^{13e} and this lack of reactivity probably rests on the weak steric intramolecular interactions between the bulky groups of the molecule. We have also attempted the orthometalation of the ylide–methanide derivatives **9–11**, but in all studied cases decomposition to Pd⁰ was observed. Probably the neutral character of these complexes provides a less electrophilic Pd center, therefore less prone to promote CH bond activations compared with **6**. Complex **12** has been characterized

through its spectroscopic data and the determination of the X–ray structure.

The IR of **12** shows a very strong absorption at 1630 cm^{–1}, shifted to higher energies with respect to **6** (1602 cm^{–1}), and in good agreement with a higher keto character. This increase has already been observed when chelating P– and N–ylides undergo orthometalation processes.^{11g,11h,13e} The NMR spectra show the presence of two sets of signals with a molar ratio (6.7/1) identical to that observed in the starting compound **6**. This means that **12** is obtained as two geometric isomers, in which the phosphine is bonded either trans to the aryl ring or trans to the ylidic carbon. Even if the PPh₃ ligand is reluctant to coordinate trans to an aryl ligand, a phenomenon known as *transphobia*^{53,54} and based on the antisymbiotic effect,⁵⁵ there are some reports in which this situation is postulated or crystallographically characterized.^{56–62} On these grounds, we have assigned the PPh₃ trans to C_{ylide} structure to the major isomer because this should be the most favorable arrangement. These spectra also show unambiguously the presence of the orthometalated unit. The ¹H NMR spectrum shows clearly four signals in the 7.0–6.5 ppm region, assigned to the C₆H₄ unit, an AB spin system around 4.5–5.5 ppm, assigned to the diastereotopic protons of the CH₂S unit, and singlets due to the ylidic protons, while the ¹³C{¹H} NMR spectrum shows six well spread peaks due to the palladated ring.

The crystal structure of **12**·CHCl₃ has been determined by X–ray diffraction methods. A drawing of the organometallic cation of **12** is shown in Figure 9, selected bond distances (Å) and angles (deg) are collected in Table 3, and the most relevant parameters concerning data collection and structure solutions and refinement are given in the Supporting Information, Table S1. The Pd atom is located in a distorted square–planar environment, surrounded by the orthopalladated carbon C(1), the ylidic carbon C(37), the chlorine Cl(1), and the phosphorus P(2). This fact confirms the metalation of the phenyl ring through CH bond activation and the formation of the sulfonium unit. The environment of the palladium center is less distorted than in **10**, since the metallacycle comprises a five membered ring. The phosphine ligand is bonded trans to the ylidic carbon C(37), and the P(1)–C(37) and S(1)–C(39) bonds are cisoid with respect to the C(38)–O(1) bond. These facts imply short P···O and S···O intramolecular contacts [3.039 Å and 2.891 Å,

(53) Vicente, J.; Arcas, A.; Bautista, D.; Jones, P. G. *Organometallics* **1997**, *16*, 2127.

(54) Vicente, J.; Arcas, A.; Gálvez–López, M. D.; Juliá–Hernández, F. *Organometallics* **2008**, *27*, 1582 and references therein.

(55) Pearson, R. G. *Inorg. Chem.* **1973**, *12*, 712.

(56) Arlen, C.; Pfeffer, M.; Bars, O.; Le Borgne, G. *J. Chem. Soc., Dalton Trans.* **1986**, 359.

(57) Villanueva, L. A.; Abboud, K.; Boncella, J. M. *Organometallics* **1991**, *10*, 2969.

(58) Singh, A.; Sharp, P. R. *J. Am. Chem. Soc.* **2006**, *128*, 5998.

(59) van Manen, H. J.; Nakashima, K.; Shinkai, S.; Kooijman, H.; Spek, A. L.; van Veggel, F. C. J. M.; Reinhoudt, D. N. *Eur. J. Inorg. Chem.* **2000**, 2533.

(60) Cámpora, J.; López, J. A.; Palma, P.; del Río, D.; Carmona, E.; Valerga, P.; Graiff, C.; Tiripicchio, A. *Inorg. Chem.* **2001**, *40*, 4116.

(61) Steffey, B. D.; Miedaner, A.; Maciejewski–Farmer, M. L.; Bernatis, P. R.; Herring, A. M.; Allured, V. S.; Carperos, V.; DuBois, D. L. *Organometallics* **1994**, *13*, 4844.

(62) Bedford, R. B.; Betham, M.; Coles, S. J.; Frost, R. M.; Hursthouse, M. B. *Tetrahedron* **2005**, *61*, 9663.

(44) Bergman, R. G. *Nature* **2007**, *446*, 391.

(45) Godula, K.; Sames, D. *Science* **2006**, *312*, 67.

(46) Bielsa, R.; Navarro, R.; Soler, T.; Urriolabeitia, E. P. *Dalton Trans.* **2008**, 1203.

(47) Bielsa, R.; Navarro, R.; Soler, T.; Urriolabeitia, E. P. *Dalton Trans.* **2008**, 1787.

(48) Aguilar, D.; Bielsa, R.; Contel, M.; Lledós, A.; Navarro, R.; Soler, T.; Urriolabeitia, E. P. *Organometallics* **2008**, *27*, 2929.

(49) Aguilar, D.; Aragüés, M. A.; Bielsa, R.; Serrano, E.; Navarro, R.; Soler, T.; Urriolabeitia, E. P. *J. Organomet. Chem.* **2008**, *693*, 417.

(50) Bielsa, R.; Navarro, R.; Lledós, A.; Urriolabeitia, E. P. *Inorg. Chem.* **2007**, *46*, 10133.

(51) Aguilar, D.; Aragüés, M. A.; Bielsa, R.; Serrano, E.; Navarro, R.; Urriolabeitia, E. P. *Organometallics* **2007**, *26*, 3541.

(52) Falvello, L. R.; Garde, R.; Miqueleiz, E. M.; Tomás, M.; Urriolabeitia, E. P. *Inorg. Chim. Acta* **1997**, *264*, 297.

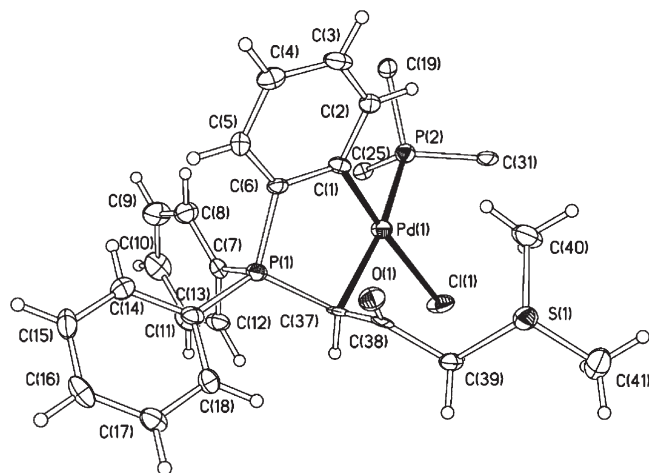


Figure 9. Thermal ellipsoid plot of the cationic fragment of complex **12**. Non-hydrogen atoms are drawn at the 50% probability level. Phenyl groups of the PPh₃ ligand (except C_{1ipso}) have been omitted for clarity.

Table 3. Selected Bond Distances (Å) and Angles (deg) for **12**·CHCl₃

Pd(1)–C(1)	1.989(3)	Pd(1)–C(37)	2.187(3)
Pd(1)–P(2)	2.2906(11)	Pd(1)–Cl(1)	2.3979(11)
C(1)–C(2)	1.388(4)	C(1)–C(6)	1.401(4)
C(2)–C(3)	1.380(4)	C(3)–C(4)	1.370(5)
C(4)–C(5)	1.382(4)	C(5)–C(6)	1.387(4)
C(6)–P(1)	1.784(3)	P(1)–C(37)	1.776(3)
C(37)–C(38)	1.433(4)	C(38)–O(1)	1.223(3)
C(38)–C(39)	1.529(4)	C(39)–S(1)	1.803(3)
S(1)–C(40)	1.781(3)	S(1)–C(41)	1.775(3)
C(1)–Pd(1)–C(37)	85.88(12)	C(1)–Pd(1)–P(2)	95.67(9)
C(37)–Pd(1)–P(2)	167.80(9)	C(1)–Pd(1)–Cl(1)	170.98(9)
C(37)–Pd(1)–Cl(1)	91.54(8)	P(2)–Pd(1)–Cl(1)	88.68(4)
C(2)–C(1)–Pd(1)	125.2(2)	C(6)–C(1)–Pd(1)	117.6(2)
C(37)–P(1)–C(6)	102.86(15)	C(38)–C(37)–P(1)	118.0(2)
C(38)–C(37)–Pd(1)	106.1(2)	P(1)–C(37)–Pd(1)	96.05(13)
O(1)–C(38)–C(37)	125.7(3)	O(1)–C(38)–C(39)	118.4(3)
C(37)–C(38)–C(39)	115.9(3)	C(38)–C(39)–S(1)	108.0(2)
C(41)–S(1)–C(40)	100.48(17)	C(41)–S(1)–C(39)	100.43(16)
C(40)–S(1)–C(39)	101.80(15)		

respectively] and dihedral angles close to zero in the case of the phosphonium unit [P(1)–C(37)–C(38)–O(1) = –7.52°, while O(1)–C(38)–C(39)–S(1) = –39.17°]. The Pd(1)–C(37) bond distance [2.187(3) Å] is identical (within experimental error) to that found in **10** and to those found on related ylides bonded to Pd(II) trans to a phosphine ligand.^{11g} The Pd(1)–C(1) bond distance [1.989(3) Å] is also identical to that found in related orthometalated complexes [1.999(8) Å].^{11g} Other internal parameters are as expected.

Conclusions

Two new species, the ylide–sulfonium salt [Ph₃PCHC(O)–CH₂SMe₂]⁺ and the ylide–sulfide [Ph₃PCHC(O)CH₂SMe],

have been prepared and fully characterized. Their deprotonation generates the bis–ylide [Ph₃PCHC(O)CHSMe₂] and the ylide–methanide [Ph₃PCHC(O)CHSMe][–] for which three different bonding modes have been characterized: neutral κ^2 -C,C for the bis–ylide, neutral κ^2 -C,S for the ylide–sulfide, and anionic κ^2 -C,C for the ylide–methanide. The coordination mode of the neutral κ^2 -C,C occur with complete diastereoselectivity for the meso form (*RS/SR*). The DFT studies (B3LYP level) on model systems of sulfur ylides [Me₂SCHC(O)R] show strong conformational preferences favoring the cisoid forms. In conjunction with Bader analysis of electron density, it was also possible to characterize the intimate nature of the phenomenon originating these preferences. The main factor responsible for the preference of the cisoid form (9.2 kcal mol^{–1}) is a set of cooperative weak-type intramolecular interactions including two 1,6-C–H···O hydrogen bonds between the protons of the methyl substituents (around 3–4 kcal mol^{–1} each) and one 1,4-S···O interaction (around 2.5 kcal mol^{–1}). These interactions are also operative in the sulfonium half of mixed P–S bis–ylides [Me₂SCHC(O)–CHPH₃], whereas a 1,4-P···O interaction is present in the phosphonium half, favoring the cisoid–cisoid structures and showing that the conformational preferences in the two halves are cooperative. Thus, the observed adoption of the meso form in the bonded mixed P–S bis–ylides is the direct result of the coordination of the cisoid–cisoid form of the free ligand, showing that the conformational preferences are preserved during the bonding process. On the other hand, the coordination modes of anionic κ^2 -C,C occur with complete diastereoselectivity but displaying the *d,l* form (*RR/SS*), which constitute a unique case since the reversed of the meso form is observed in the formation of bis–ylides.

Acknowledgment. Funding by the Ministerio de Ciencia e Innovación (MICINN) (Spain, Projects CTQ2008-01784, CTQ2008-06549-C02-01/BQU, and CTQ2008-06866-C02-01) is gratefully acknowledged. E.S. thanks the Diputación General de Aragón (Spain) for a Ph.D. research grant.

Supporting Information Available: Complete experimental section with all preparative data and references, table of crystallographic parameters of data collection and refinement, table of energetic and geometric parameters for bisylides [H₃PCHC(O)CHSMe₂] (**14**) and the corresponding C,C-chelating complexes (**15**), potential energy profiles for [Me₂SCHC(O)Me], Cartesian coordinates of computed cisoid (**c**), transition state (**TS**) and transoid (**t**) structures of ylide [Me₂SCHC(O)Me] (**13**), bisylides (**14**) and the corresponding complexes (**15**). This material is available free of charge via the Internet at <http://pubs.acs.org>.